LBL-17866
Preprint c.2

Lawrence Berkeley Laboratory

UNIVERSITY OF CALIFORNIA

RECEIVED
LAWRENCE
BERKELEY LABORATORY
AUG 20 1984
LIBRARY AND
DOCUMENTS SECTION

Engineering & Technical Services Division

Submitted to Review of Scientific Instruments

140 GHz PULSED FOURIER TRANSFORM MICROWAVE SPECTROMETER

W.F. Kolbe and B. Leskovar

May 1984

TWO-WEEK LOAN COPY
This is a Library Circulating Copy
which may be borrowed for two weeks.

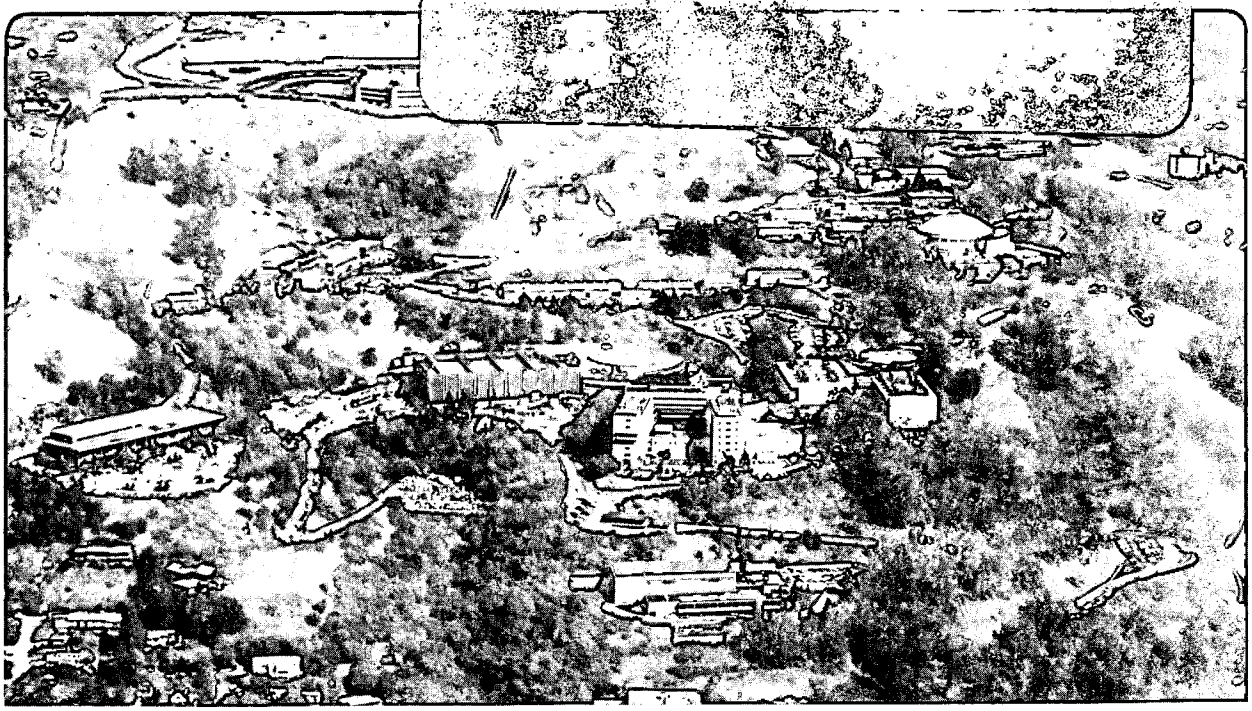

LBL-17866
c.2

Prepared for the U.S. Department of Energy under Contract DE-AC03-76SF00098

DISCLAIMER

This document was prepared as an account of work sponsored by the United States Government. While this document is believed to contain correct information, neither the United States Government nor any agency thereof, nor the Regents of the University of California, nor any of their employees, makes any warranty, express or implied, or assumes any legal responsibility for the accuracy, completeness, or usefulness of any information, apparatus, product, or process disclosed, or represents that its use would not infringe privately owned rights. Reference herein to any specific commercial product, process, or service by its trade name, trademark, manufacturer, or otherwise, does not necessarily constitute or imply its endorsement, recommendation, or favoring by the United States Government or any agency thereof, or the Regents of the University of California. The views and opinions of authors expressed herein do not necessarily state or reflect those of the United States Government or any agency thereof or the Regents of the University of California.

LBL-17866
May 15, 1984

140 GHz PULSED FOURIER TRANSFORM MICROWAVE SPECTROMETER

W.F. Kolbe and B. Leskovar

Lawrence Berkeley Laboratory
University of California
Berkeley, California 94720 U.S.A.

A pulsed microwave spectrometer operating in the vicinity of 140 GHz for the detection of rotational transitions in gaseous molecules is described. The spectrometer incorporates a tunable Fabry-Perot cavity and a subharmonically pumped superheterodyne receiver for the detection of the molecular emission signals. A 70 GHz source supplying a high efficiency frequency doubler which is pulse modulated at 30 MHz produces sidebands of sufficient power at 140 GHz to excite the molecules. The cavity is tuned to one of the modulation sidebands. The operation of the spectrometer is illustrated by the detection of emission signals from the 6(2,4)-6(1,5) transition of SO_2 gas. The generation of the electric dipole analog of NMR "spin-echo" signals by a $\pi/2$-π pulse sequence is also described.

INTRODUCTION

In contrast to steady-state microwave spectroscopy, in which molecular species are detected by their equilibrium absorption of microwave energy, pulsed Fourier transform spectroscopy exploits the transient polarization of the molecules produced by a brief pulse of microwave energy at a frequency in the vicinity of the transition. The polarized molecules emit a polarization decay signal at their resonance frequency, which is detected by a sensitive microwave receiver. The decay signals from a number of pulses are then digitized and signal averaged to enhance the signal-to-noise ratio. Subsequently the time domain signal can be Fourier transformed to obtain the resonance lineshape. The method is directly analogous to that employed in pulsed NMR experiments and has many of the advantages associated with that technique.

In recent years pulsed microwave spectrometers have been developed[1-3] which have demonstrated the usefulness of the method. However, these have, for the most part, been limited to operating frequencies of less than 18 GHz because of the unavailability at higher frequencies of microwave switches suitable for forming the polarizing pulses. The requirements for the pulse forming switch include an on/off ratio of 100 dB or more[1] and a risetime of a few ns. Commercial pin diode switches[4] are currently available with on/off ratios of up to 60 dB for frequencies as high as 50 GHz. These units, however, have bandwidths of only a few percent, making them very expensive for spectroscopic applications. Wider bandwidth switches operating at frequencies up to 110 GHz have ratios of less than 20 dB and are not suitable.

In the present spectrometer we take a different approach to generate the necessary polarizing pulses. Instead of using a switch to directly control the microwave power, we use a modulated frequency doubler to generate sideband frequencies of sufficient power to excite the molecules. The modulation is then switched on and off with a conventional low frequency switch to generate

the pulses. With this arrangement, on/off ratios in excess of 90 dB are readily achieved. Since the modulation process introduces sidebands above and below the carrier in addition to the carrier itself, a high-Q tunable transmission cavity is employed both as the sample cell and as a filter to pass only the desired frequency.

In the following section we describe the components and operation of the spectrometer. In Section II we demonstrate the detection of transient emission signals using SO_2 gas as a sample species and, in Section III, investigate the combination of pulse widths and power necessary to produce the optimum polarization. Finally we demonstrate the use of double pulse excitation of the gas to generate polarization echos.

I. EXPERIMENTAL APPARATUS

A block diagram of the spectrometer is shown in Fig. 1. The major components in the system include a 70 GHz microwave source, a modulated frequency doubler to provide excitation pulses at 140 GHz, a subharmonically pumped receiver to detect the gas emission signal and a Fabry-Perot transmission cavity containing the sample gas.

Microwave power in the vicinity of 70 GHz is produced by a klystron which is phase-locked to a frequency synthesizer. Of the approximately 80 mW of power available from the source, ten percent is used to provide local oscillator power for the receiver and the remainder is employed to drive the frequency doubler.

To provide sufficient pulse power to polarize the gas molecules, a tunable high efficiency frequency doubler was used. This doubler was constructed according to a design[5] furnished by the National Radio Astronomy Observatory and had a conversion efficiency of at least 15% over an output frequency range of 130 to 146 GHz. The doubler was provided with an appropriate d.c. bias to

maximize the output power and simultaneously modulated[6] at 30 MHz at the same port. The resulting signal thus consisted of the doubled carrier plus side-bands 30 MHz above and below the carrier. The maximum output power generated in each of the sidebands was measured (using the Fabry-Perot as a tunable filter) and found to be greater than 1 mW. To pulse the modulation on and off, a Watkins-Johnson model S1 switch was used to provide an on/off ratio of greater than 90 dB and a risetime of 1 ns.

The carrier frequency and both sidebands were fed to a tunable Fabry-Perot cavity[6,7] consisting of two opposing mirrors 5 cm in diameter, one flat and the other spherical, mounted in a vacuum chamber. Two coupling waveguides are attached to the flat mirror through electroformed coupling holes 4.0 mm apart and 0.7 mm in diameter. The spherical mirror has a radius of curvature of 14.8 cm and is mounted in a semi-confocal configuration with a distance of about 7.4 cm between the two mirrors. The cavity can be tuned by moving the spherical mirror with the use of a piezoelectric transducer and a stepping motor and micrometer drive provided for this purpose. The loaded Q of the cavity was about 73000 and the transmission loss through the cavity was approximately 18 dB. Because of the high quality factor of the cavity, only one sideband from the modulated frequency doubler passes through the cavity and reaches the receiver. By appropriately tuning the cavity to the desired value, either sideband can be detected.

After passing through the cavity the microwave signal is converted to an IF frequency of 30 MHz by the receiver. A subharmonically pumped mixer[8] with a noise figure of 12.5 dB (DSB) was used to permit the 70 GHz source frequency to be used directly as a local oscillator. Alternatively, a second frequency doubler and a fundamental mixer could have been used. After preamplification, the receiver output signal is passed thorugh a gating switch (a Hewlett-Packard 10514A mixer) to prevent saturation of the IF amplifier during the polarization pulse. The IF signal is then converted to baseband frequency

by means of a phase detector driven by the same 30 MHz source used with the modulator. A phase shifter is used to obtain the in-phase component of the cavity signal. The detected signal is then digitized using an 8-bit Transiac model 2008 transient digitizer, a CAMAC-based unit with a maximum sampling rate of 20 MHz and a memory size of up to 8K channels. A PDP-11/34 computer is used to average the digitized data from a number of pulse sequences and to further process the data.

To generate the necessary signals to drive the pulse and gating switches and to trigger the transient digitizer, a pulse sequencer, incorporating two Advanced Micro Devices Am 9513 timing controller chips, was constructed. It was fashioned after the design described in Ref. 9 and was interfaced to the CAMAC system. Because the Am 9513 was operated with a 5 MHz clock, the available pulse widths were limited to multiples of 200 ns. In order to provide a finer control of the pulse widths, a pulse generator with variable width controls and triggered by the sequencer, was optionally employed. For the double pulse experiments described below, two pulse generators were used as shown with their outputs connected together.

In order to illustrate the generation of transient emission signals, the cavity was filled with SO_2 gas at a pressure of a few mTorr. The microwave frequency was set to 140.3062 GHz corresponding to the 6(2,4)-6(1,5) transition of the gas[10] and the cavity was tuned to resonate at that frequency. The mechanical stability of the cavity was sufficient to maintain its frequency at resonance during individual experiments with only infrequent retuning. The excitation pulse width was set to a convenient value between 500 and 1000 ns and the 30 MHz modulation power adjusted to maximize the amplitude of the emission signal.

Figure 2 shows the cavity excitation pulse and the transient emission signal at the output of the receiver preamplifier for a gas pressure of 7 mTorr and a pulse width of 500 ns. Although the rectangular input pulse also shown

is distorted by the cavity time constant, it has been demonstrated[11] that the polarization produced is proportional to the integral of the pulse to first order independant of this distortion. In order that the molecular emission signal be observed, the cavity decay time must be short compared to the molecular relaxation time. The voltage decay time is given by $\tau_c = 2Q_L / \omega_0$ where Q_L is the cavity loaded Q and ω_0 is the frequency. For our cavity τ_c is approximately 175 ns.

In order to display the transient emission signal, the output of the receiver was further amplified, phase detected and digitized as described above. Figure 3 shows the result for an average of 1000 scans taken at a pressure of 1.0 mTorr. The excitation pulse begins at t=0 and, as shown in the figure, extends for 400 ns. A short time later the receiver gating signal is turned off, permitting the tail of the cavity decay and the oppositely phased emission signal to be observed. In this figure the excitation frequency has been chosen to correspond exactly to the rotational transition frequency. If the frequency is shifted by 2 MHz as shown in Fig. 4, the emission signal appears as a damped sinewave of that frequency. In either case, the lineshape in the frequency domain can be recovered by Fourier transformation.

The time dependance of the emission signal has been shown in Ref. 11 to have the functional form:

$$E(t) = E_0 \exp(-t/T_2) \exp(-t^2/4q^2) \qquad (1)$$

Here, T_2 is the polarization relaxation time arising from molecular collisions and q is the Doppler dephasing time resulting from the Boltzmann distribution of molecular velocities. T_2 can be expressed[11] in terms of the low power collision broadened linewidth, $\Delta\nu$, as

$$T_2 = 1/(2\pi\Delta\nu) \tag{2}$$

Using the value of $(\Delta\nu)_1$ = 15.6 MHz/Torr which we measure for this transition, one obtains for a pressure of 1 mTorr, T_2 = 10.2 μs. The quantity q is given by the expression[11]:

$$q = (\ln 2)^{1/2}/\Delta\omega_D \tag{3}$$

where for a given temperature, T, molecular mass, m, and frequency, ω_o, the Doppler half width, $\Delta\omega_D$ is

$$\Delta\omega_D = \frac{\omega_o}{c}\left(\frac{2kT\ \ln 2}{m}\right)^{1/2} \tag{4}$$

For SO_2 at 140 GHz and ambient temperatures, q = 1.2 μs. Figure 3 shows the calculated decay signal obtained with E_o = 21 mV, T_2 = 10.2 μs and q = 1.15 μs in good agreement with these values.

II. EMISSION AMPLITUDE AS A FUNCTION OF $\kappa\varepsilon_o\tau_p$

The amplitude of the transient emission signal is a function[11] of the applied electric field, the pulse length, τ_p, and the transition matrix element and, as in the analogous pulsed NMR case, is a maximum when the quantity $\kappa\varepsilon_o\tau_p$ is approximately equal to $\pi/2$. In this expression, $\kappa = 2\hbar^{-1}|\langle a|\mu_z|b\rangle|$ where $\langle a|\mu_z|b\rangle$ is the electric dipole matrix element and ε_o is defined in terms of the peak electric field as $\varepsilon_o = E_o/2$. In the Fabry-Perot cavity the gas molecules do not experience a uniform electric field and the total polarization must be obtained by an integration over the field distribution in the cavity. It is shown in Ref. 11 that the emission amplitude is then approximately given as

$$I = I_0 \frac{1 - J_0(\kappa\varepsilon_0\tau_p)}{\kappa\varepsilon_0\tau_p} \tag{5}$$

where J_0 is the Bessel-function of order 0.

The above expression for the emission amplitude is only valid if the transition is non-degenerate. In the case of the 6(2,4)-6(1,5) transition of SO_2, the rotational quantum number, J=6 and there are 2J+1=13 degenerate M-states comprising the transition. Since each of these M-states have differing transition matrix elements[12], Eq. 5 must be summed over these to obtain the total contribution to the intensity. Figure 5 shows the predicted amplitude of the emission signal as a function of $\kappa\varepsilon_0\tau_p$ for both the degenerate and non-degenerate cases. As can be seen, the effect of including the 13-fold degeneracy is to wash out the oscillations of the Bessel function and to introduce a small shift in the peak position.

In order to compare the predicted intensity variation with experiment, measurements of the amplitude of the emission signal were made at differing pulse power levels and for three different pulse widths, 0.5, 1.0 and 1.5 μs. The results are shown in Fig. 6. Since the electric field in the cavity is proportional to the square root of the microwave power at the cavity input, the product $(P_{in}^{1/2})\,\tau_p$ is plotted against the intensity for each of the three cases. A Hughes 140 GHz bolometer was used to estimate the microwave power. The fact that the peak amplitude occurs at the same position for each of the three pulse widths is good evidence of the validity of Eq. 5 in explaining the present results. It was derived[11] assuming a short pulse limit for τ_p, and the decrease in the peak amplitude observed with the 1.5 μs pulse is most likely due to a violation of this condition.

The magnitude of the electric field in the cavity can be estimated from the known cavity Q, the transmission loss at the input and output ports and a measurement of the microwave power level at the input of the cavity. This was

done using an equation similar to that present in Ref. 11. The resulting electric field calculated for the peak emission signal was about 1.8 times that predicted by the theory and shown in Fig. 5, not a very large error considering the uncertainties involved in the measurements.

III. TWO PULSE ECHO MEASUREMENTS

In pulsed nuclear magnetic resonance experiments, the spin-echo technique[13] has been used extensively to measure the nuclear relaxation time T_2 under conditions where the free induction decay signal (FID) is dominated by local magnetic field inhomogeneities. In these experiments, a $\pi/2$ pulse is used to polarize the nuclear spin system and, after the FID signal has disappeared, a second π pulse of twice the duration is applied. An echo signal, of amplitude determined by T_2, then occurs at a time after the second pulse equal to the difference in the two pulse times.

As McGurk, Schmalz and Flygare have shown[14], a similar behavior is predicted to occur for the electric dipole transitions associated with molecular rotational states. Their calculations, derived for the case of a traveling plane wave excitation, yield the following result for the emitted electric field following the second pulse:

$$\begin{aligned} E(t) = &- \frac{\pi h \kappa \omega l \Delta N_0}{2c} e^{-(t-3t_1)T_2} \\ &\times \{ e^{-(t-3t_1)^2/4q^2} \cos\left[\omega_0(t-3t_1)+3\omega t_1-kz\right] \\ &+ e^{-(t-t_1-2t_2)^2/4q^2} \cos\left[\omega_0(t-2t_2-t_1)+\omega(2t_2+t_1)-kz\right] \} \end{aligned} \tag{6}$$

In this equation, the first pulse of duration t_1 occurs at time $t=0$ and is followed at time $t=t_2$ by a pulse of duration $2t_1$. The echo given by the second term of the equation, then occurs at time $t = 2t_2+t_1$. The first term is the tail of the transient emission signal from the first pulse. No

transient emission signal is produced by the second π-pulse. As in the single pulse experiment described above, the quantity q is the Doppler dephasing time. Its role is similar to that played by the magnetic field inhomogeneity in the NMR case. Only if $T_2 > q$ can echos be observed.

To demonstrate the production of echo signals the cavity was filled with SO_2 at a pressure of 0.5 mTorr. The pulse sequencer was then programmed to generate a double pulse signal with the duration of each pulse being controlled by a triggered pulse generator as shown in the block diagram. After adjusting the duration of the first pulse to maximize the amplitude of the transient emission signal ($\pi/2$-pulse), the second pulse was adjusted to maximize the echo amplitude (π-pulse). The result is shown in Fig. 7 where echos for three different delay times are presented. In this plot the position of the second pulse is held fixed while the time of the first pulse is varied. In addition, the receiver is gated off during the two pulses to prevent saturation of the spectrometer. The small excitation pulses shown in the figure are thus greatly attenuated from their actual values. As can be seen, in each case the echo occurs at a time after the second pulse equal to the time between pulses. It should be noted that, in the case of a strong echo, a second, much weaker echo of opposite phase occurs at three times the pulse separation. The mechanism producing this echo is not understood, although it may be due to additional polarization produced by the electric field built up in the cavity during the primary echo.

The duration of the first pulse in the above experiment was 360 ns while, for the second pulse, a length of 520 ns produced the maximum echo amplitude. The ratio between the two pulse lengths was thus less than a factor of two. This deviation from the ideal $\pi/2$-π ratio is most likely due to the fact that the molecules are subjected to a range of electric fields as they move through the cavity. While the plane wave theory summarized in Eq. 6 predicts no transient emission signal following the second pulse, one is actually pro-

duced as can be seen from Fig. 7. This further illustrates the fact that a true π-pulse cannot be produced in the Fabry-Perot cavity.

We have plotted in Fig. 8, on a logarithmic scale, the echo amplitudes measured for three different gas pressures as a function of the elapsed time after the first pulse. The decay times for these measurements are summarized in the accompanying Table I. In each case the observed decay times are shorter than the T_2 relaxation times calculated from the pressure broadened linewidth using the equation given previously. This is due to the presence of an additional decay mechanism not accounted for in Eq. 6 which arises because the molecules, which are moving with a high velocity, leave the region of the cavity, where the electric field is large, before they can be collisionally relaxed. To properly account for this effect, a more complete calculation following the methods of Ref. 11 is needed. However, a rough interpretation of the results can be made by defining a characteristic residence time, $T_d = 25.4\ \mu s$ for the molecules given by the ratio of the average waist radius (0.79 cm) of the Gaussian cavity beam[15] to the mean kinetic velocity (3.1×10^4 cm/s). Then we have

$$\frac{1}{T_{corr}} = \frac{1}{T_{obs}} - \frac{1}{T_d} \qquad (7)$$

where T_{corr} is the corrected relaxation time. The results which are presented in Table I are in reasonable agreement with the calculated values for T_2.

IV. DISCUSSION

The general theory of transient effects in microwave spectroscopy has been worked out in detail[14] by Flygare and coworkers. In addition, these principles have been applied[11] to the special case of pulsed excitation in a

Fabry-Perot cavity. However, spectrometers using these techniques have in the past been limited to operating frequencies below 18 GHz. By incorporating a pulse modulated frequency doubler as a polarizing source, we have extended the operation of such spectrometers to the short millimeter range.

We have demonstrated the operation of the spectrometer by detecting the emission signals produced by an SO_2 rotational transition and showed that the conditions for optimum pulse excitation can be readily obtained with the pulse generation scheme we have employed. In addition we have demonstrated that, as previously observed in the infrared region[16], polarization echos can be produced using double pulse excitation.

The technique should be of interest to workers investigating coherent transient phenomena in the millimeter region[17] where transitions are stronger than they are at low frequencies and for investigations of short-lived species which have absorption lines at these frequencies. In addition we hope to use the spectrometer together with a pulsed supersonic molecular beam capable of rotationally cooling the molecular species to provide greater sensitivity. This technique has been used very successfully[2] at lower frequencies.

ACKNOWLEDGEMENTS

This work was performed as part of the program of the Electronics Research and Development Group of the Department of Instrument Science and Engineering, of the Lawrence Berkeley Laboratory, and was supported by the Director's Office of Energy Research, Office of Health and Environmental Research of the U.S. Department of Energy under Contract DE-AC03-76SF00098. Reference to a company or product name does not imply approval or recommendation of the product by the University of California or the U.S. Department of Energy to the exclusion of others that may be suitable.

The authors would like to express their appreciation to Dr. John Archer and Mr. Niel Horner of the National Radio Astronomy Observatory and to Mr. Ronald Forsythe and Mr. Stan Halpern of the Georgia Institute of Technology for their assistance in the fabrication of the frequency doubler and the subharmonically pumped mixer used in these experiments.

TABLE I. Two pulse echo relaxation data for SO_2 6(2,4)-6(1,5) transition at 140.306 GHz

Pressure (mTorr)	T_{obs} (μs)	T_{corr}[a] (μs)	T_2 (μs)
1.61	5.5	7.1	6.3
1.05	7.1	9.9	9.7
0.51	11.0	19.6	20.0

[a] $1/T_{corr} = 1/T_{obs} - 1/T_a$ with $T_d = 25.4$ μs.

REFERENCES

1. J. Ekkers and W.H. Flygare, Rev. Sci. Instrum., 47, 448 (1976).

2. T.J. Balle and W.H. Flygare, Rev. Sci. Instrum., 52, 33 (1981).

3. A.C. Legon and L.C. Willoughby, Chem. Phys., 74, 127 (1983).

4. For example, 1984 Millimeter Wave Catalog, Alpha Industries, Woburn, MA.

5. J.W. Archer, IEEE Trans. Microwave Theory Tech., MTT-29, 552 (1981).

6. W.F. Kolbe and B. Leskovar, Rev. Sci. Instrum., 53, 769 (1982).

7. W.F. Kolbe and B. Leskovar, Int. J. Infrared Millimeter Waves, 4, 733, (1983).

8. Mixer fabricated by the Denver Research Institute and Georgia Institute of Technology.

9. H. Saint-Jalmes and Y. Barjhoux, Rev. Sci. Instrum., 53, 1 (1982).

10. F.J. Lovas, J. Phys. Chem., Ref. Data, 7, 1445 (1978).

11. E.J. Campbell, L.W. Buxton, T.J. Balle and W.H. Flygare, J. Chem. Phys., 74, 813 (1981).

12. C.H. Townes and A.L. Schawlow, Microwave Spectroscopy, McGraw-Hill, New York, 1955.

13. E.L. Hahn, Phys. Rev., 80, 580 (1950).

14. J.C. McGurk, T.G. Schmalz and W.H. Flygare, Adv. Chem. Phys., XXV, 1 (1974).

15. H. Kogelnik and T. Li, Proc. IEEE, 54, 1312 (1966).

16. R.L. Shoemaker in Laser and Coherence Spectroscopy, J.I, Steinfeld, ed., Plenum Press, New York 1978.

17. M.D. Blue, P.B. Reinhard, and J.J. Gallagher, Int. J. Infrared Millimeter Waves, 1, 255 (1980).

FIGURE CAPTIONS

Fig. 1 Block diagram of pulsed spectrometer.

Fig. 2 Cavity excitation pulse and transient emission signal for pulse width of 500 ns and gas pressure 7 mTorr.

Fig. 3 Transient emission signal for SO_2 at 1.0 mTorr and frequency offset of 0 MHz. 400 ns pulse ends at time, t_p and receiver gating is disabled at time, t_1. Dashed line shows calculated decay with E_0 = 21 mV, T_2 = 10.2 μs and q = 1.15 μs.

Fig. 4 Transient emission signal for SO_2 at 1.0 mTorr and frequency offset of 2.0 MHz. t_p and t_1 as in Fig. 3.

Fig. 5 Calculated transient emission amplitude as a function of $\kappa\varepsilon_0\tau_p$ for (—— - -), non-degenerate transition and (——), degenerate transition with J = 6.

Fig. 6 Measured transient emission amplitude as a function of $P_{in}^{1/2}\tau_p$.

Fig. 7 Measured $\pi/2-\tau-\pi$ pulse echo signals for SO_2 at 0.5 mTorr and three different pulse separations, (a) τ = 9.3 μs, (b) τ = 12.5 μs and (c) τ = 15.7 μs.

Fig. 8 Semi-log plot of echo amplitude as a function of total elapsed time after the first pulse for three different SO_2 gas pressures.

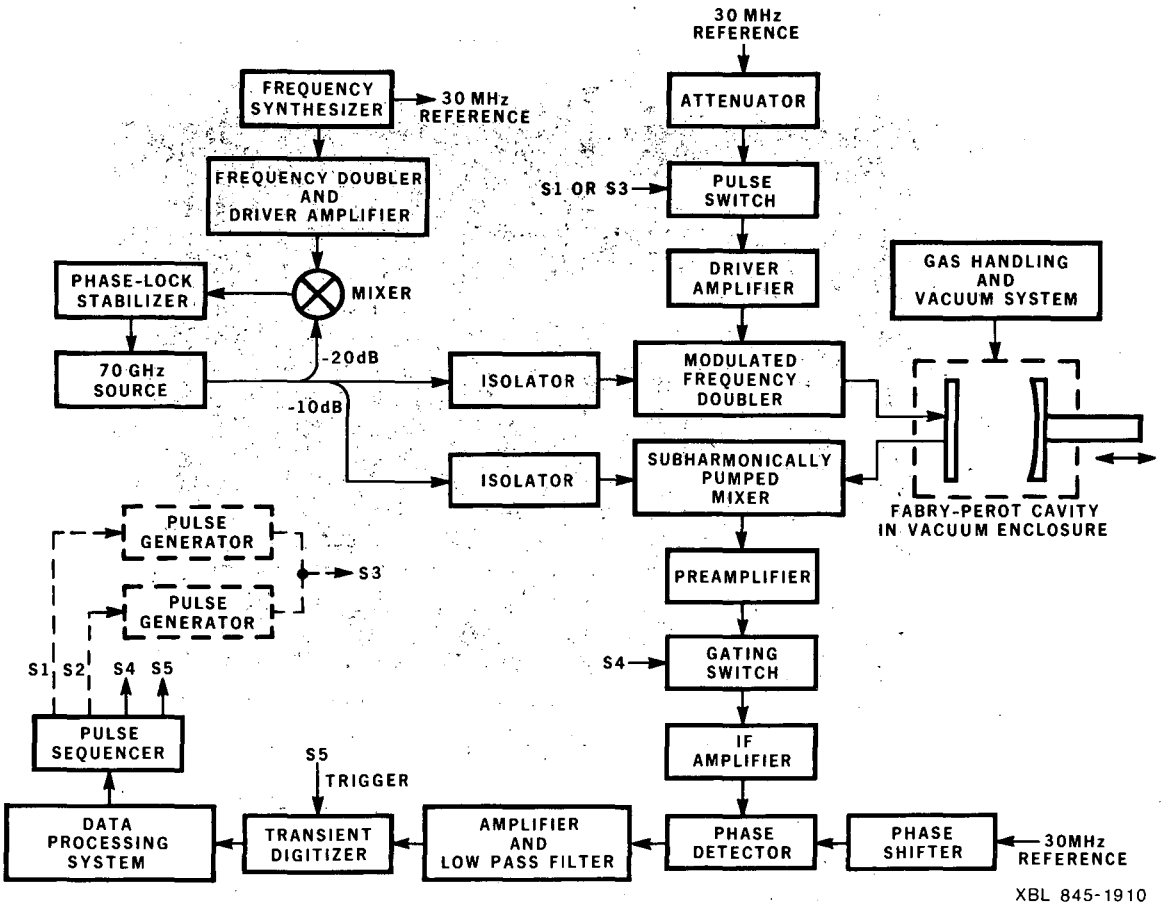

Fig. 1 Block diagram of pulsed spectrometer.

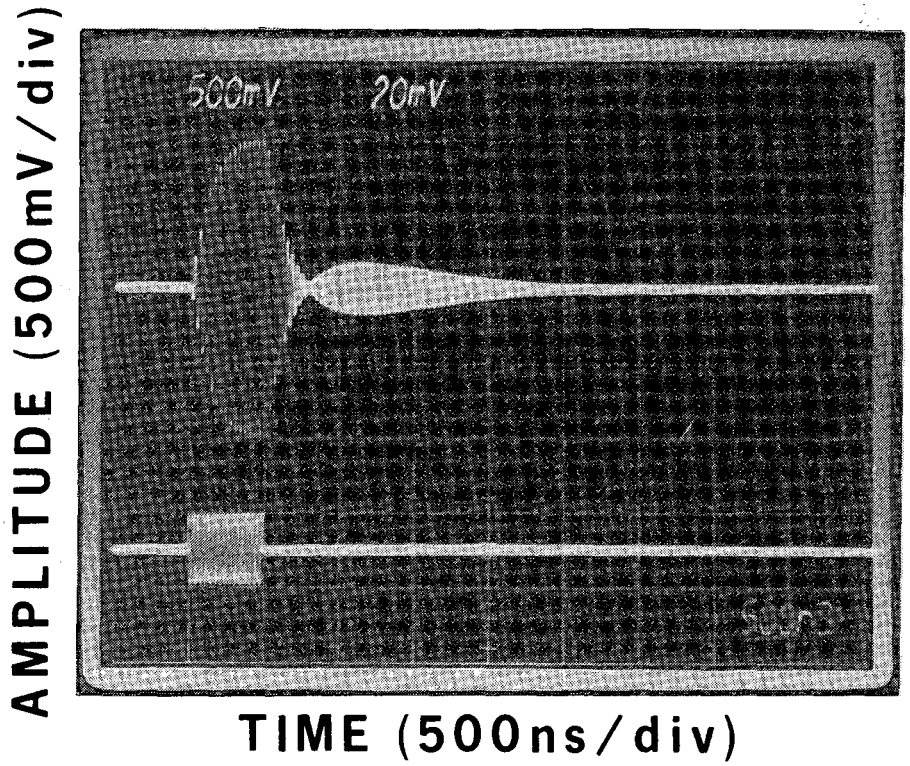

Fig. 2 Cavity excitation pulse and transient emission signal for pulse width of 500 ns and gas pressure 7 mTorr.

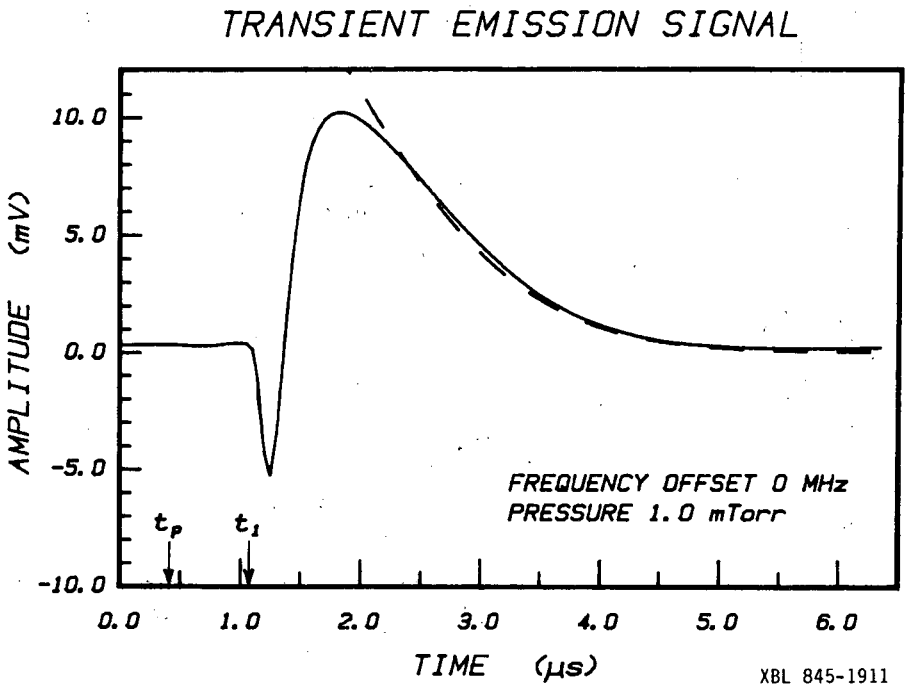

Fig. 3 Transient emission signal for SO_2 at 1.0 mTorr and frequency offset of 0 MHz. 400 ns pulse ends at time, t_p and receiver gating is disabled at time, t_1. Dashed line shows calculated decay with E_0 = 21 mV, T_2 = 10.2 μs and q = 1.15 μs.

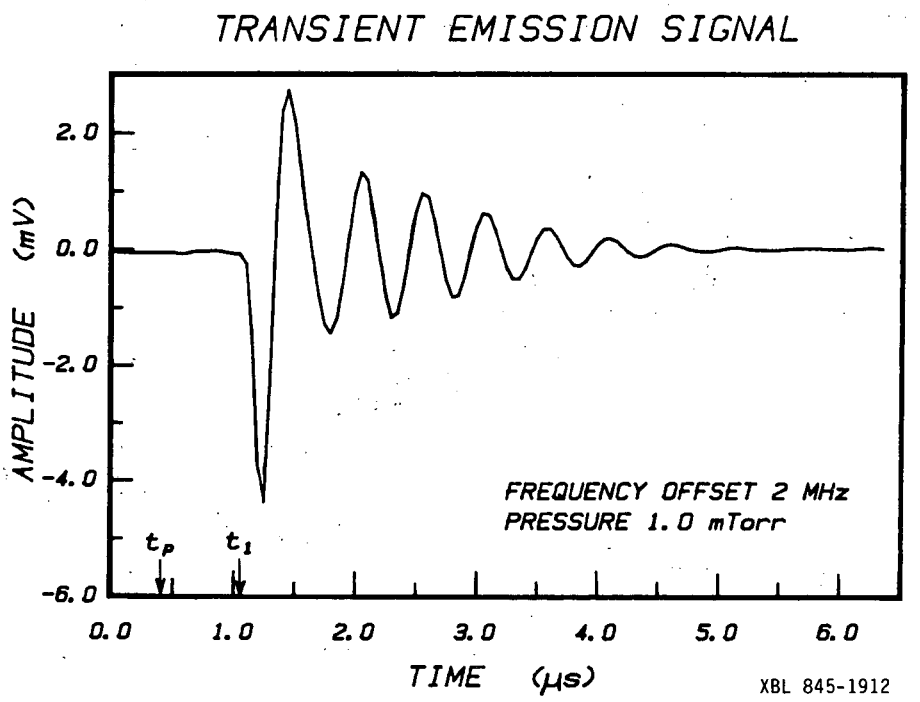

Fig. 4 Transient emission signal for SO_2 at 1.0 mTorr and frequency offset of 2.0 MHz. t_p and t_1 as in Fig. 3.

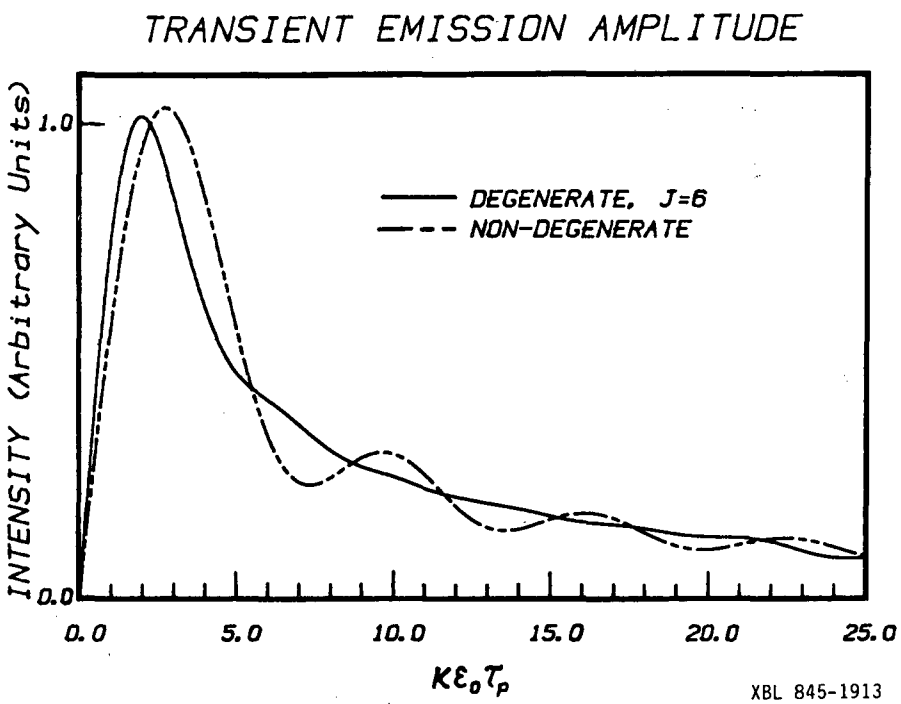

Fig. 5 Calculated transient emission amplitude as a function of $\kappa\varepsilon_0\tau_p$ for (——— — —), non-degenerate transition and (———), degenerate transition with J = 6.

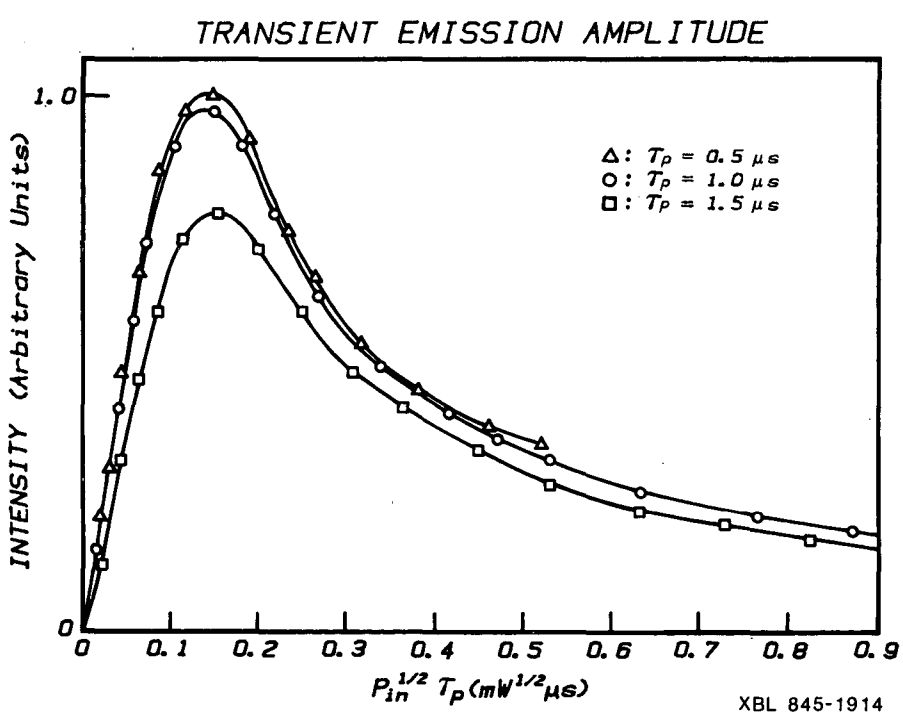

Fig. 6 Measured transient emission amplitude as a function of $p_{in}^{1/2}\,\tau_p$.

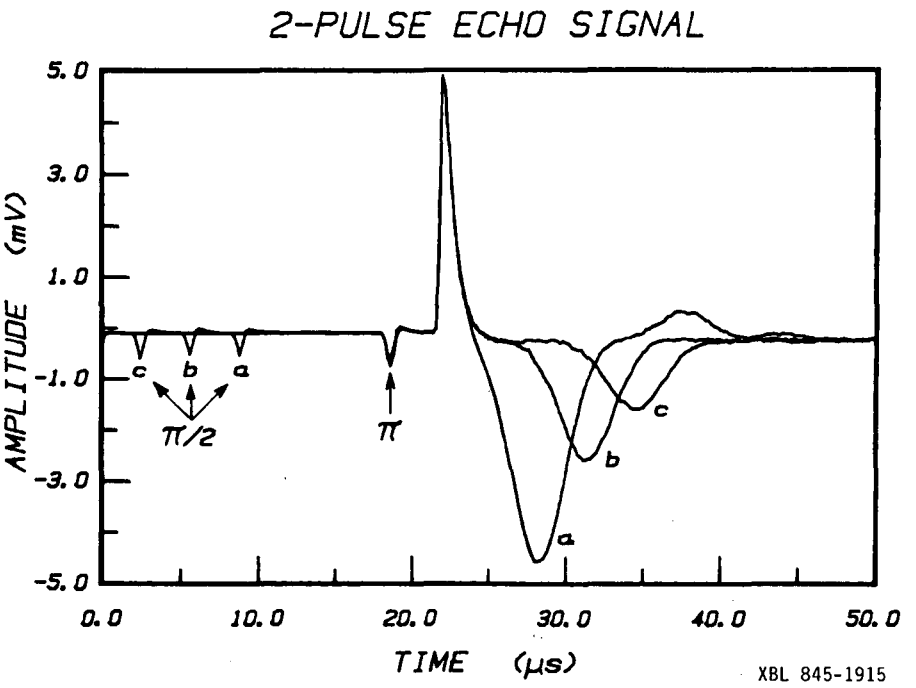

Fig. 7 Measured $\pi/2$-τ-π pulse echo signals for SO_2 at 0.5 mTorr and three different pulse separations, (a) τ = 9.3 μs, (b) τ = 12.5 μs and (c) τ = 15.7 μs.

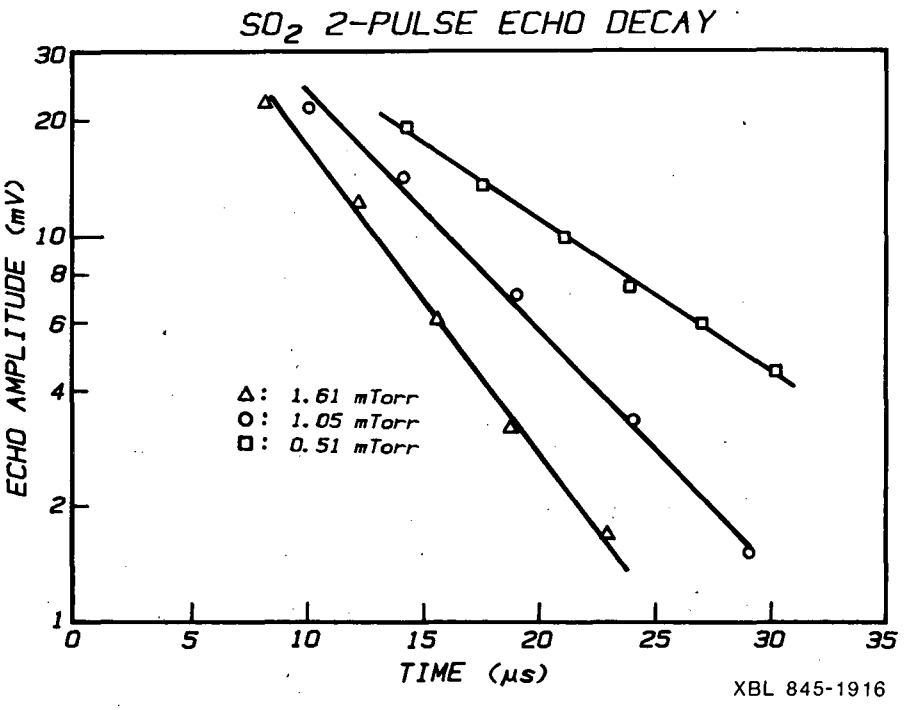

Fig. 8 Semi-log plot of echo amplitude as a function of total elapsed time after the first pulse for three different SO_2 gas pressures.

This report was done with support from the Department of Energy. Any conclusions or opinions expressed in this report represent solely those of the author(s) and not necessarily those of The Regents of the University of California, the Lawrence Berkeley Laboratory or the Department of Energy.

Reference to a company or product name does not imply approval or recommendation of the product by the University of California or the U.S. Department of Energy to the exclusion of others that may be suitable.

TECHNICAL INFORMATION DEPARTMENT
LAWRENCE BERKELEY LABORATORY
UNIVERSITY OF CALIFORNIA
BERKELEY, CALIFORNIA 94720